Effect of Solute Concentration on Hindered Diffusion in Porous Membranes

Jiahui Shao and Ruth E. Baltus
Dept. of Chemical Engineering, Clarkson University, Potsdam, NY 13699

The effect of solute concentration on hindered diffusion was investigated by measuring diffusion rates of dextran and polyethylene glycol (PEG) in track-etched polycarbonate membranes at concentrations up to 60 mg/mL. Results were interpreted using a model that incorporates a first-order virial coefficient to describe the concentration dependence of the equilibrium partition coefficient, as well as the intrapore diffusivity. For dextran, both virial coefficients were positive, indicating that the effective diffusivity increases with solute concentration. Measured values of the virial coefficient for equilibrium partitioning agreed with a model that includes attractive van der Waals interactions between dextran and the pore wall. For PEG, both virial coefficients were negative, indicating that the diffusivity decreases as solute concentration increases. These observations may be due to chain entanglement or aggregation that occurs with increasing PEG concentration.

Introduction

The effective diffusion coefficient of a solute within a pore of comparable size is usually found to be less than its value in the bulk solution. This phenomenon is called hindered diffusion. Most of the previous work investigating various aspects of hindered diffusion has focused on the infinite dilution limit, where solute-solute interactions are neglected. In general, the membrane is treated as an array of cylindrical pores and the solute is assumed to have both Brownian and hydrodynamic characteristics. For spherical solutes in an unbounded fluid, this leads to the Stokes-Einstein equation

$$D_{\infty,o} = k_B T/6\pi\mu r_s \tag{1}$$

where $D_{\infty,o}$ is the bulk solution diffusion coefficient under infinite dilution condition (cm^2/s), k_B is Boltzmann's constant (1.38×10^{-16} J/K), T is absolute temperature (K), μ is the solvent viscosity ($N\cdot s/m^2$), and r_s is the hydrodynamic radius of the solute (cm).

The reduced diffusion coefficients that are typically observed with membrane separations arise from the combined effect of: (1) solute partitioning between the pore and bulk solutions; (2) an increase in the hydrodynamic drag experienced by the solute in the pore relative to that experienced in an unbounded fluid. These effects are combined when defining an effective diffusion coefficient

$$D_{\text{eff}} = K_{\text{eq}} D_p \tag{2}$$

where K_{eq} is the equilibrium partition coefficient and D_p is the intrapore diffusivity (cm^2/s). Much of the theoretical and experimental research in this field is summarized in a review article by Deen (1987).

For many applications where hindered diffusion plays an important role, solute concentration is sufficiently large so that intermolecular interactions cannot be neglected. Graessley (1980) estimated that polymer chains begin to significantly interact at molar concentrations exceeding $(8\ N_A\ r_g^3)^{-1}$, where N_A is Avogadro's number and r_g is the radius of gyration of the polymer. For dextran with a molecular weight of 40,000, this corresponds to a solution concentration less than 20 mg/mL. In gel permeation chromatography experiments, several studies have shown that the equilibrium partition coefficient increases with bulk solution concentration (Cantow et al., 1966; Rudin, 1971; Bleha et al., 1977; Satterfield et al., 1978). Measurements by Satterfield et al. (1978) of polystyrene diffusion through porous glass showed that the partition co-

Correspondence concerning this article should be addressed to R. E. Baltus.

efficient increases with bulk-phase concentration, at first in a linear fashion and then more gradually at higher concentrations. These observations were explained by proposing that the mean dimensions of the macromolecule decrease as concentration increases, leading to a reduction in the steric limitations imposed by the pore wall. However, this explanation does not apply to compact macromolecules whose dimensions are relatively fixed.

The effect of solute concentration on the equilibrium partition coefficient has been modeled using a virial expansion approach (Glandt, 1981; Anderson and Brannon, 1981; Post and Glandt, 1985), linear density functional theory (Post, 1989), a low-dimensional approximation (Glandt, 1981; Post, 1989; Post and Kofke, 1992), semi-grand-canonical Monte Carlo simulations (Post and Kofke, 1992), and a Gibbs ensemble Monte Carlo method (GEMC) (Chun and Phillips, 1997). For bulk solute concentrations less than 10.9 vol. %, the virial expansion results are nearly identical to those obtained by both the GEMC method and linear density functional theory for values of the solute to pore-size ratio less than 0.6 (Chun and Phillips, 1997). For solute/pore size ratios greater than 0.6, GEMC results agree with the low-dimensional approximations.

Anderson and Brannon (1981) developed a model for the concentration dependence of the distribution coefficient for rigid spherical macromolecules in cylindrical and slit pores. They viewed equilibrium partitioning from a statistical thermodynamic framework utilizing the McMillan-Mayer assumption, which neglects changes in solvent-macromolecule interactions as concentration is changed. The partition coefficient is expressed as a virial expansion in bulk solution concentration

$$K_{\mathrm{eq}} = K_{\mathrm{eq},o}\left[1 + \alpha_1 \phi_\infty + \alpha_2 {\phi_\infty}^2 + \ldots\right] \tag{3}$$

where $K_{\mathrm{eq},o}$ is the partition coefficient at infinite dilution, ϕ_∞ is the volume fraction of solute in the bulk solution, and the coefficients α_j are virial coefficients which depend on configurational integrals involving $j+1$ macromolecules and the pore wall. Knowing solute and pore size, the results of Anderson and Brannon (1981) can be used to predict α_1 when only steric interactions govern the partitioning. Their results predict positive values of α_1, indicating that K_{eq} increases with increasing ϕ_∞. Calculations were also presented for systems in which electrostatic interactions between solutes, and between solutes and the pore wall, are significant.

An experimental investigation of concentration effects on the partitioning of dextrans and bovine serum albumin was conducted by Brannon and Anderson (1982) using porous glass beads. The results for bovine serum albumin were in reasonable agreement with hard-sphere theory predictions. However, the K_{eq} values measured for dextran were significantly smaller than the hard-sphere theory predictions, although values were observed to increase with increasing solute concentration. In making this comparison, the hydrodynamic (Stokes Einstein) radius was used to describe the dextran size. Polydispersity of the dextran samples was proposed as a possible explanation for these observations.

Anderson and Adamski (1983) and Mitchell and Deen (1984) theoretically investigated the effect of solute concentration on ultrafiltration. In their analyses, it was assumed that solute concentration only affects solute partitioning and that solute-solute hydrodynamic interactions are negligible when compared to solute-pore wall hydrodynamic interactions. Results from both studies predict that the membrane rejection coefficient for rigid macromolecules decreases with increasing bulk concentration. Mitchell and Deen (1986) measured rejection coefficients for ficoll and bovine serum albumin in track-etched polycarbonate membranes and their experimental results showed the expected decrease in rejection coefficient as solute concentration increases. However, experimentally measured rejection coefficients were considerably larger than those predicted by the theory, an observation that was attributed to solute adsorption effects.

An evaluation of the effect of solute-solute interactions on intrapore transport coefficients has not been previously reported. However, the effect of solute concentration on bulk-phase diffusion has been theoretically and experimentally investigated. Theoretically, two approaches have been adopted (Selim and Al-Naafa, 1993). The first is a statistical-mechanical approach and is based on the N-particle Smoluchowski equation, which describes the instantaneous N-particle distribution function in configuration space. The second approach was most notably applied by Batchelor (1976) who extended Einstein's thermodynamic argument of sedimentation-diffusion equilibrium to finite concentrations and derived a formal expression for the Brownian diffusion coefficient in bulk solution. In describing the effect of solute-solute interactions on diffusion in bulk solution, Batchelor considered two effects. One arises from the fact that when solutions are not infinitely dilute, there is an enhancement in the diffusivity because there are more free sites available to a diffusing solute in a region of lower concentration, when compared to a region of higher concentration. The second effect is hydrodynamic and arises because solvent near a solute particle is dragged with the solute. To ensure continuity, solvent farther from the solute is backwashed in the direction opposite to the direction of solute movement. Neighboring solute particles cannot sample the solution near the particle because of steric exclusion. Therefore, the hydrodynamic effect causes a reduction in the diffusivity as neighboring particles experience the backwash. For spherical solutes in bulk solution restricted to hard-sphere interactions, Batchelor predicted that the excluded volume effect overcomes the hydrodynamic effect, yielding a first virial coefficient of 1.45

$$D_\infty = D_{\infty,o}\left[1 + 1.45\phi_\infty + O\left({\phi_\infty}^2\right)\right] \tag{4}$$

where D_∞ is the solute diffusion coefficient in bulk solution at finite concentration (cm^2/s). Berne and Pecora (1976) used a similar approach but found the $O(\phi_\infty)$ coefficient to be 0.45. Beenakker and Mazur (1982) considered three-body interactions in their analysis and found the $O(\phi_\infty)$ coefficient to be 1.56. There have been reports from a large number of other theoretical studies based on both approaches with predictions for the first virial coefficient ranging from -2.6 to $+3$ (Selim and Al-Naafa, 1993).

Experimental investigations which test these theories are few and also contradictory. The majority of these experimental studies were carried out on microemulsions, polymer lat-

Table 1. Pore Length and Density of Nuclepore Membranes Determined from Scanning Electron Microscopy Images

Nominal Size (μm)	Pore Length (μm)	Pore Density (Pores/cm$^2 \times 10^{-8}$)
0.1	5.80	3.28
0.05	5.81	5.66
0.03	5.95	5.35

tices and proteins in high ionic strength buffers, and silica dispersions in nonpolar solvents. Results from many of these studies are summarized in Selim and Al-Naafa (1993). Quite different values for the $O(\phi_\infty)$ coefficient have been reported with values ranging from -5.2 to $+1.39$.

In order to interpret transport measurements at high concentration, an accurate prediction of solute diffusion at low concentration conditions is needed. The effective diffusion coefficients of narrow size range fractions of dextran and polyethylene glycol (PEG) were measured under infinite dilution conditions in our laboratory using track-etched polycarbonate membranes (Shao, 2000; Shao and Baltus, 2000). The measured diffusivities were found to be larger than those predicted for a rigid sphere, as well as for a flexible polymer when solutes are restricted to steric interactions with the pore wall. The measured effective diffusion coefficient values were successfully interpreted using a model that includes van der Waals attractive interactions between the solute and the pore wall. Results indicated that there was negligible adsorption of dextran and PEG to the pore wall, as well as insignificant electrostatic interactions between solute and the pore wall.

In this article, we report the results of an experimental examination of the effect of solute concentration on hindered diffusion of dextran and PEG. Results are interpreted using a model that incorporates a first-order virial expansion in concentration for both the equilibrium partition coefficient and the intrapore diffusivity. Measured virial coefficients are compared to those predicted by previously developed theoretical models for the effect of concentration on partitioning and on bulk phase diffusion.

Experimental Studies

Track-etched Nuclepore polycarbonate membranes with nominal pore radii of 0.1, 0.05, and 0.03 μm were obtained from Corning Separation Division (Corning Costar, Acton, MA). The pore density and pore length were determined from scanning electron microscopy (SEM) images collected using a JEOL JSM-6300 scanning electron microscope. The pore radius of each membrane was determined by measuring the hydraulic (water) permeability of each membrane before and after a diffusion experiment. The measured pore length and pore density of membranes used in this study are summarized in Table 1. Details of the membrane characterization methods are reported elsewhere (Shao, 2000).

For both polymers, all solutions were prepared using water which was distilled and filtered through a 0.1 μm membrane. Polyethylene glycol (PEG) with weight-average molecular weight of 10890 was obtained from Pressure Chemical Co. (Pittsburgh, PA). The manufacturer reported that polydispersity of this sample was 1.19. This polymer was used as received without further fractionation.

Dextran T40 with weight-average molecular weight of approximately 40000 and dextran T70 with weight-average molecular weight of approximately 70000 were obtained from Pharmacia (Piscataway, NJ). The polydispersity index of these materials is about 1.5. Because hindered diffusion rates are sensitive to solute size, the polydispersity of the polymer sample can have a significant effect on measured diffusion coefficients. For our experiments performed under infinite dilution conditions, dextran fractions with a narrow molecular weight distribution were obtained from these materials using preparative gel permeation chromatography (Shao and Baltus, 2000). However, it would be very time-consuming and not practical to use the same approach for this study because it would be necessary to collect a significant amount of fractionated polymer. Therefore, an alternative approach was developed to measure diffusion rates of narrow size range dextran fractions and a description of this approach follows.

Solutions were prepared using T40 and T70 dextrans as received and each diffusion experiment was actually a multicomponent diffusion experiment. In order to identify the diffusion coefficient of an approximately monodisperse fraction, the collected dextran samples were analyzed using analytical scale gel permeation chromatography (GPC) to obtain the molecular weight distribution of each sample. This was done using a system comprised of a Waters model 600E HPLC

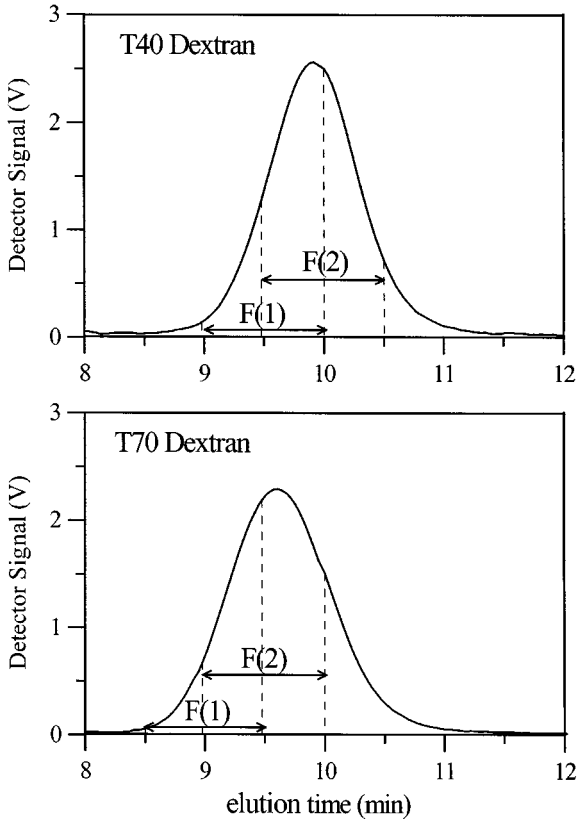

Figure 1. Molecular size distribution for T40 and T70 Dextrans obtained using GPC on Shodex KB-80M column.

F(1) and F(2) refer to the two narrow size distribution fractions identified for diffusion measurements.

Table 2. Properties of Dextran Fractions and PEG

Solute	$\overline{M}_w$	$\overline{M}_n$	$\frac{\overline{M}_w}{\overline{M}_n}$	$D_{\infty,0}$ ($cm^2/s \times 10^7$)	$r_s^{\ddagger}$ (nm)
Dextran					
T40:F(1)	27,300*	23,300*	1.17	5.3†	4.6
T40:F(2)	50,600*	43,800*	1.16	4.0†	6.1
T70:F(1)	59,000*	51,500*	1.15	3.7†	6.6
T70:F(2)	107,500*	93,900*	1.14	2.8†	8.7
PEG	10,890**	9,150**	1.19	8.2§	3.0‡

*Determined by gel permeation chromatography analysis using ASTM standard method D3536-91 (Shao, 1999).
**Reported by Pressure Chemical Corporation
†Obtained from light scattering measurements performed at Clarkson University.
‡Stokes-Einstein radius determined from $D_{\infty,0}$ and Eq. 1.
§Using expression derived by Singh et al. (1998) from intrinsic viscosity relationship.

solvent delivery system, a Waters model 410 refractive index detector and a Shodex Ohpak KB-80M gel column (8 mm ID × 300 mm). The voltage signal from the detector was sent via a data acquisition system to a personal computer using a Basic program.

The GPC column was calibrated using monodisperse dextran standards (Waters) with peak molecular weight 196,000, 124,000, 43,500, 21,400, 9,900, and 4,400. A good straight line calibration was achieved when a semilog plot of dextran molecular weight vs. retention volume was prepared. The operating conditions for the GPC analysis of the dextran samples collected from the diffusion experiments were the same as those used for the column calibration.

The chromatograms obtained from a GPC analysis of the T40 and T70 dextrans are shown in Figure 1. In each chromatogram, two fractions were identified and are labeled as F(1) and F(2) in Figure 1. Values of $\overline{M}_w$ and $\overline{M}_n$ of each fraction were determined using the calibration prepared using the monodisperse dextrans and ASTM standard method D3536-91. The properties of each fraction are listed in Table 2. The polydispersity of each fraction was smaller than 1.2.

Dextran and PEG diffusion experiments at finite concentrations were performed using a glass diaphragm diffusion cell that is described in detail elsewhere (Shao, 2000). It consists of two half-cells, one with a volume of 12.64 cm^3, and the other with a volume of 15.87 cm^3. The membrane, supported by a stainless steel screen support, was sandwiched between the two half cells. The cell was stirred internally by Teflon coated bar magnets which were acted upon by a magnet external to the cell. The diffusion cell was jacketed for water circulation to maintain a constant temperature (25.0 ± 0.1°C).

The procedure used for the diffusion experiments is shown in Figure 2. Initially, one reservoir was filled with a high concentration solution while the opposite chamber was filled with distilled and filtered water. In order to simplify the analysis of the experimental data, the solute concentration in the high concentration reservoir was kept constant by continuously feeding this reservoir with fresh polymer solution at a flow rate of about 12 mL/h. The solute concentration in the low concentration reservoir was monitored by removing samples at discrete intervals during the course of the experiment. This was done by injecting water into one port and collecting a sample from the effluent from another port. The sampling

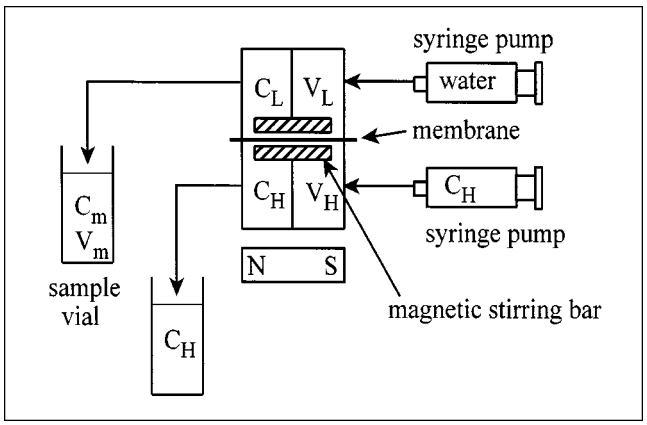

Figure 2. Experimental system used for diffusion experiments.

Diffusion cell was constructed of glass and was jacketed to allow for circulation of constant temperature water.

flow rate was set at about 0.9 mL/min and samples were collected for one minute. Valves were closed in the low concentration reservoir between sampling. The collected sample was weighed to determine its volume and analyzed using gel permeation chromatography. At least five samples were collected during each diffusion experiment. The concentration of each fraction in the low concentration reservoir at the start of each sample collection period was related to the measured sample concentration by a mass balance on the sampling process, assuming ideal stirred reservoir behavior

$$C_{L,t} = C_m \frac{V_m}{V_L}\left[1 - \exp(-V_m/V_L)\right]^{-1} \tag{5}$$

where $C_{L,t}$ is the solute concentration of the fraction of interest in the reservoir at the beginning of the sampling (mg/mL), C_m is the volume averaged (measured) concentration of that fraction for a sample (mg/mL) with volume V_m and V_L is the volume (mL) of the low concentration reservoir. Two samples were removed from the high concentration cell, one at the start and one at the end of each experiment, to determine C_H and to ensure that it was constant during the experiment.

The absolute concentration of each fraction in each collected sample was not determined because only the relative concentration $\phi_L/\phi_H{}^o$ was needed for our analysis. Results from preliminary experiments showed that the refractive index of dextran and PEG solutions are proportional to solute concentration up to the maximum solution concentration used for these experiments. Therefore, for each fraction, the ratio ϕ_L/ϕ_H^o was assumed to be equal to the ratio of the areas under respective GPC elution profiles, with limits for each fraction as shown in Figure 1.

In order to check the validity of this method for sample analysis, several dextran diffusion experiments were conducted under infinite dilution conditions and the results were compared to those obtained with fractionated dextrans with polydispersity index smaller than the 1.2 obtained from preparative gel permeation chromatography. The effective diffusion coefficients obtained from the partial peak area

concentration analysis were found to be in good agreement with values obtained using fractionated dextrans (Shao, 2000). This confirms that this procedure and analysis method are valid for determining the diffusion coefficients of narrow size range dextran fractions.

For experiments at finite concentration, a material balance on solute in the low concentration reservoir yields

$$V_L \frac{d\phi_L}{dt} = -\frac{n\pi r_p^2}{\ell} \int_{K_H \phi_H}^{K_L \phi_L} D_p(\phi_p)\, d\phi_p \tag{6}$$

where ϕ_p is the intrapore volume fraction of solute, ϕ_L is the volume fraction of solute in the low concentration cell, ϕ_H is the volume fraction of solute in the high concentration cell, and K_L and K_H are the equilibrium partition coefficients at each side of the membrane. When deriving Eq. 6, it was assumed that there were no boundary layer resistances external to the membrane, an assumption that was confirmed with independent measurements (Shao, 2000). The concentration dependence of the intrapore diffusivity is assumed to follow a virial expansion in ϕ_p

$$D_p = D_{p,o}\left[1 + \beta_1 \phi_p + \beta_2 \phi_p^2 + \ldots\right] \tag{7}$$

where $D_{p,o}$ is the intrapore diffusivity at infinite dilution conditions (cm^2/s). The concentration dependence of K_L and K_H are assumed to follow a virial expansion in bulk solution concentration

$$K_L = K_{eq,o}\left[1 + \alpha_1 \phi_L + \alpha_2 \phi_L^2 + \ldots\right] \tag{8}$$

$$K_H = K_{eq,o}\left[1 + \alpha_1 \phi_H + \alpha_2 \phi_H^2 + \ldots\right] \tag{9}$$

A substitution of Eqs. 7, 8, and 9 into Eq. 6 and setting $\phi_H = \phi_H^0$ yields

$$V_L \frac{d\phi_L}{dt} = \frac{n\pi r_p^2 K_{eq,o} D_{p,o}}{\ell} \left[\left[\phi_H^o - \phi_L\right] + \left[(\phi_H^o)^2 - \phi_L^2\right] \times \left(\alpha_1 + \frac{\beta_1 K_{eq,o}}{2}\right) + \left[(\phi_H^o)^3 - \phi_L^3\right] \times \left(\alpha_1 \beta_1 K_{eq,o} + \alpha_2 + \frac{\beta_2 K_{eq,o}^2}{3}\right) + O\left[(\phi_H^o)^4 - \phi_L^4\right]\right] \tag{10}$$

where terms of $O(\phi^4)$ and higher were neglected. All the parameters in Eq. 10 were known except the virial coefficients. The membrane parameters n, r_p, and ℓ were known from membrane characterization measurements. The hindered diffusion coefficient $D_{p,o}$ and the equilibrium partition coefficient $K_{eq,o}$ were obtained using the model that was developed from results obtained at infinite dilution that incorporates attractive van der Waals interactions between the solute and the pore wall (Shao, 2000; Shao and Baltus, 2000). In order to determine values for the first-order coefficients α_1 and β_1, it was assumed that $\alpha_2 + \beta_2 K_{eq,o}^2/3 = 0$. The validity of this assumption is discussed later in this article.

For each fraction, best fit values for α_1 and β_1 were determined using a least-squares fitting procedure. This data fitting procedure involved minimization of the function $\Sigma(\phi_{L,pred} - \phi_{L,meas})^2$ where the summation was performed over the data collected for one diffusion experiment. Here, $\phi_{L,pred}$ is the sample concentration predicted from a numerical integration of Eq. 10 and $\phi_{L,meas}$ is the measured sample concentration of the fraction of interest. The data fitting was carried out using a program written in Maple V.

The units of concentration used in Eqs. 6–10 are solute volume fractions, because this is the convenient concentration unit used in theoretical predictions of α_1. In order to convert the convenient experimental concentration units of mg/mL into volume fraction, the specific volume of the solute must be known. For each solute, the specific volume was estimated from the bulk phase diffusivity using the Stokes-Einstein equation (Eq. 1). For dextran, the bulk-phase diffusion coefficient was determined in water at 25°C using dynamic light scattering. A power law relationship between $D_{\infty,o}$ and the weight average molecular weight was developed, and this relationship was then used with Eq. 1 to develop a relationship between the effective hydrodynamic radius and the weight average molecular weight (Shao, 2000). The specific volume was then estimated from r_s using the definition of ν_2

$$\nu_2 = \frac{4}{3}\pi r_s^3 \frac{N_A}{M} \tag{11}$$

In their study of dextran partitioning, Brannon and Anderson (1982) were able to relate volume fraction and mass fraction concentrations using the second osmotic virial coefficient, which was determined from osmotic pressure measurements. The specific volume of dextran calculated using Eq. 11 is in reasonable agreement with the volume derived from the osmotic virial coefficient values reported by Brannon and Anderson, indicating that dextran is not swollen by solvent to an appreciable extent under the conditions of these measurements.

For PEG, the bulk-phase diffusivity was determined from a power law relationship developed by Singh et al. (1998) from a relationship for intrinsic viscosity (Shao, 2000). The specific volume was then determined from this relationship and Eqs. 1 and 11.

Results

Dextran

Dextran T70 diffusion experiments were conducted using solutions with dextran concentrations of 19.9 mg/mL, 42.2 mg/mL, and 59.6 mg/mL in 0.1 μm and 0.05 μm pore-size membranes. Dextran T40 diffusion experiments were performed using solutions with a concentration of 42.2 mg/mL in 0.1 μm and 0.05 μm membranes.

The values of α_1 and β_1 determined by a data fit of the dextran concentration vs. time data are summarized in Table 3. The relationship between the first virial coefficient for the equilibrium partition coefficient (α_1) and the dimensionless solute size ($r_s/r_p = \lambda$) is shown in Figure 3. The first virial coefficient for the intrapore diffusivity (β_1) is plotted as a function of λ in Figure 4. In presenting these results, the Stokes-Einstein radius is used to describe the solute size.

Table 3. Measured Values of α_1 and β_1 for Dextrans in 0.1 μm and 0.05 μm Membranes

Conc. (mg/mL)	$r_{p,avg}^{*}$ (μm)	Dextran	$\lambda = r_s/r_{p,avg}$	α_1	β_1
19.89	0.0911	T70:F(1)	0.072	0.28	0.28
		T70:F(2)	0.096	0.39	0.36
	0.0521	T70:F(1)	0.127	0.52	0.46
		T70:F(2)	0.168	0.75	1.08
42.19	0.0921	T70:F(1)	0.072	0.27	0.26
		T70:F(2)	0.095	0.37	0.30
	0.0526	T70:F(1)	0.125	0.50	0.45
		T70:F(2)	0.166	0.81	0.92
	0.0526	T70:F(1)	0.125	0.59	0.51
		T70:F(2)	0.166	0.72	1.01
	0.0868	T40:F(1)	0.053	0.17	0.25
		T40:F(2)	0.070	0.36	0.31
	0.0505	T40:F(1)	0.091	0.39	0.33
		T40:F(2)	0.121	0.47	0.47
59.64	0.0894	T70:F(1)	0.074	0.27	0.26
		T70:F(2)	0.098	0.42	0.30
	0.0507	T70:F(1)	0.130	0.55	0.43
		T70:F(2)	0.173	0.73	0.95

*Average of pore radius determined from water permeability measurements performed before and after the diffusion experiment.

For dextran, all values of α_1 and β_1 were found to be positive, indicating that the effective diffusion coefficient increases with bulk solution concentration. The experimental results for both α_1 and β_1 show internal consistency with different solution concentrations and molecular weight fractions. Note, for example, the close agreement in both α_1 and β_1 values determined for the T70 F(2) fraction in the smallest pore membrane ($\lambda = 0.17$) for experiments conducted at each of the concentration levels. This internal consistency is also illustrated by the close agreement between α_1 and β_1 values determined for the T70 F(1) fraction, and the T40 F(2) fraction for $\lambda = 0.125$ and the T70 F(2) and T40 F(1) fractions with $\lambda = 0.1$. This consistency confirms the assumption

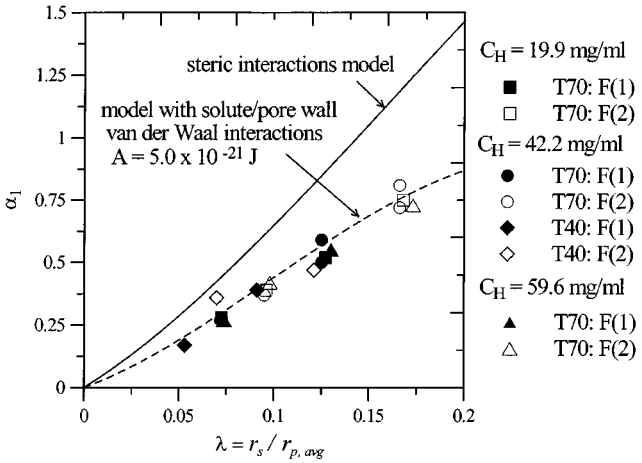

Figure 3. First virial coefficient for equilibrium partitioning for Dextran as a function of dimensionless solute size.

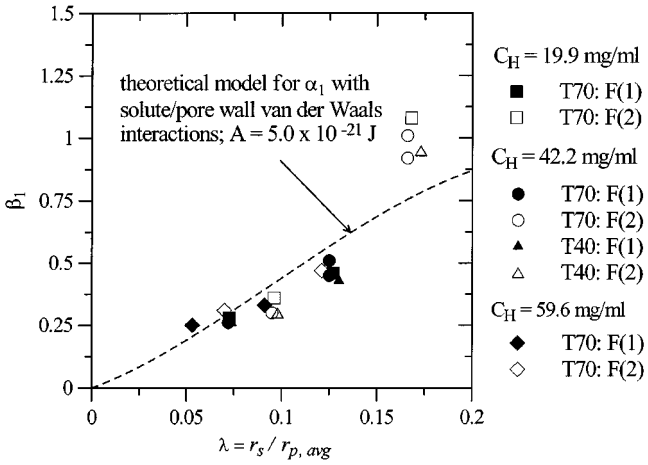

Figure 4. First virial coefficient for the intrapore diffusivity for Dextran as a function of dimensionless solute size.

that the concentration dependence of both the equilibrium partition coefficient and the intrapore diffusivity can be described using a virial expansion in solution concentration and supports our assumption that $\alpha_2 + \beta_2 K_{eq,o}^2 / 3 = 0$.

Polyethylene-Glycol

Diffusion experiments were conducted using PEG solutions with concentrations of 18.6 mg/mL and 40.0 mg/mL using 0.03 μm pore-size membranes. For each experiment, α_1 and β_1 values were obtained by a data fit of the concentration vs. time data and the values are listed in Table 4.

All the values for α_1 and β_1 were found to be negative. Experimental values of α_1 and β_1 were reasonably close with different solute concentrations, although more scatter was observed with the PEG results than was observed with the results found for dextran.

Discussion

Dextran

In Figure 3, experimental values of α_1 are compared to values predicted by Anderson and Brannon (1981) for a hard-sphere solute with only steric solute-solute and solute-pore wall interactions considered. It is clear that the experimental values of α_1 are smaller than those predicted by Anderson and Brannon for the same λ. Brannon and Anderson (1982) also experimentally investigated the effect of concentration on the equilibrium partition coefficient of dextran in porous glass using a batch mass balance technique. It was found that the measured partition coefficient increased with bulk-phase concentration and the relationship appeared to be linear up to 50 mg/mL. In their experiments, T40, T70, and T500 dextrans were used, yielding systems with $\lambda = 0.2$ to 2.0. These dimensionless solute sizes are larger than those used for our measurements, making it impossible to directly compare our results to theirs. However, their measured values of α_1 were also much smaller than the hard-sphere theory predictions. The polydispersity of the dextran samples ranged from 1.5 to 2.7, and it was proposed that this polydis-

Table 4. Measured Values of α_1 and β_1 for the PEG ($\bar{M}_w$ = 10,890) in 0.03 μm Membrane (λ = 0.094)

Conc. (mg/mL)	α_1	β_1
18.6	−0.40	−0.38
40.0	−0.33	−0.35

persity was responsible for the difference between their measured values of α_1 and those predicted for hard spheres. In our study, the polydispersity of the dextran and PEG was less than 1.2. Therefore, the effects of solute polydispersity are not expected to be significant.

Results from our previously reported study of dextran diffusion at infinite dilution conditions showed that a model incorporating attractive van der Waals interactions between a spherical solute and the pore wall was needed to explain the experimental results (Shao, 2000; Shao and Baltus, 2000). In an attempt to explain our experimental observations for α_1, a model was developed to relate α_1 to λ which includes attractive van der Waals interactions between the solute and the pore wall.

Following the approach presented by Anderson and Brannon (1981), the model development begins with a virial expansion in bulk concentration for the single-particle distribution function in a restricted environment where the effect of the porous medium is represented by a position-dependent potential energy acting on each macromolecule. The key to explaining the concentration effect on the distribution function is to appreciate the coupling between solute-solute and solute-pore wall interactions that occurs in the relevant configurational integrals appearing in an activity expansion of the grand partition function.

One considers a system containing solute particles with radius r_s, which are free to exchange between the bulk and pore regions. The partition coefficient K_{eq} is defined as

$$K_{eq} \equiv \left[\frac{\phi_p}{\phi_\infty}\right]_{eq} \tag{12}$$

where ϕ_p is the average particle volume fraction in the pore based on the volume accessible to the solvent, and ϕ_∞ is the particle volume fraction in the bulk solution. The distribution coefficient may be related to the single particle distribution, also known as the time-averaged local particle volume fraction within the pore $\phi(x)$ by

$$K_{eq} = \frac{\int_V \phi(x)\,dx}{\phi_\infty} \tag{13}$$

where V is the volume of the pore. Positions in the pore are denoted by x and dx is the corresponding volume element.

The single particle distribution function can be written in virial form using configurational integrals (McQuarrie, 1976) and relates $\phi(x)$ to the potential energies in the system

$$\frac{\phi(x)}{\phi_\infty} = \exp\left[-E(x)/k_BT\right]\left[1 + b_1(x)\phi_\infty + O\left(\phi_\infty^2\right)\right] \tag{14}$$

The interaction energy between a single particle whose center is at x and the pore wall is $E(x)$ and the function $b_1(x)$ represents the simultaneous particle-particle and particle-pore wall interactions. The function $b_1(x)$ can be written as

$$b_1(x) = \int_V \left[f_{1P}\, f_{10}\right] dx_1 \tag{15}$$

$$f_{10} = \exp\left[-U(|x - x_1|)/k_BT\right] - 1$$

$$f_{1P} = \exp\left[-E(x_1)/k_BT\right] - 1$$

where $U(|x - x_1|)$ is the pair potential acting between two particles, one located at position x and the other at x_1.

The interaction energies can have both steric and long-range components

$$E = \begin{cases} \infty & \text{(steric exclusion)} \quad r > r_p - r_s \\ E(r) & \qquad\qquad\quad r < r_p - r_s \end{cases} \tag{16}$$

$$U = \begin{cases} \infty & \text{(steric exclusion)} \quad x_{ij} < 2r_s \\ U(x_{ij}) & \qquad\qquad\quad x_{ij} > 2r_s \end{cases} \tag{17}$$

where x_{ij} is the center-to-center distance between two particles and $E(r)$ is the van der Waals attractive interaction energy between a particle at radial position r and the pore wall. Bhattacharjee and Sharma (1995) have reported semi-analytical results for the van der Waals interactions between a spherical particle and a cylindrical pore. Their results show that, when $\lambda < 0.2$, the interaction energy between a sphere and the wall of a cylindrical pore can be reasonably approximated by an expression for a sphere interacting with a flat plate. Since λ was less than 0.2 in this study, we have used the simpler expression for a sphere interacting with a plate that was given by Hamaker (1937)

$$E(x) = \frac{A}{12}\left\{\frac{1}{g} + \frac{1}{g+1} + 2\ln\frac{g}{g+1}\right\} \tag{18}$$

$$g = \frac{1 - \beta - \lambda}{2\lambda}$$

where A is the Hamaker constant (J) which characterizes the interaction between the solute and the polycarbonate membrane in water and β is the dimensionless radial position of the solute in the pore r/r_p. When particles are inside the pore, the mean particle-particle spacing is larger than in the bulk solution. Therefore, the average long-range particle-particle interaction energy was assumed to be much smaller than the long-range particle-pore wall interaction energy and $U(x_{ij})$ was assumed to equal 0 when performing the calculation for b_1.

The function $b_1(x)$ (Eq. 15) can be separated into a steric contribution $b_1^{(S)}$, plus a long-range contribution $b_1^{(LR)}$

$$b_1 = b_1^{(S)} + b_1^{(LR)} \tag{19}$$

$$b_1^{(S)} = \int\int\int \begin{pmatrix} r_1 > r_p - r_s \\ x_{10} < 2r_s \end{pmatrix} r_1\, dr_1\, d\theta_1\, dz_1 \tag{20}$$

$$b_1^{(LR)} = -\int\int\int \begin{pmatrix} r_1 < r_p - r_s \\ x_{10} < 2r_s \end{pmatrix} \{\exp[-E(r)/k_B T] - 1\} \times r_1\, dr_1\, d\theta_1\, dz_1 \quad (21)$$

If the interactions are only steric ($E(r) = 0$), then $b_1^{(LR)} = 0$. Determination of $b_1^{(S)}$ from Eq. 20 involves finding the intersection of a sphere of radius r_s centered at r (the position of the base particle) with a long cylinder of radius $r_p - r_s$ (cm). That is, the test particle (subscript 1) is moved around a large volume V of the system, and only the volume that is simultaneously excluded by the base particle and the pore wall is counted. Our calculated values of $b_1^{(S)}$ agree with those reported by Anderson and Brannon (1981). The long-range contribution $b_1^{(LR)}$ was determined by integrating Eq. 21 using Eq. 18 for $E(r)$ with $A = 5.0 \times 10^{-21}$J. This value for the Hamaker constant was determined from an appropriate average of the literature values for the individual materials in vacuum (Hiemenz and Rajagopalan, 1997; Shao, 2000). This value for A also provided excellent agreement between theory and experiments for the dextran and PEG diffusion coefficients measured at infinite dilution conditions (Shao and Baltus, 2000). Values for b_1 were then calculated using Eq. 19.

Comparing Eq. 12 and Eq. 14, one obtains

$$\alpha_1 = K_{\text{eq},o}^{-1} \langle b_1(x) \exp[-E(x)/k_B T] \rangle \quad (21)$$

where the angular bracket denotes an average over the pore volume V. Values of $b_1(x)$ were integrated over the pore volume to obtain α_1 for various values of λ. The numerical integration was performed using a Newton-Cotes algorithm, which is an internal function in Maple V. Table 5 summarizes the values of α_1 calculated with only steric interactions and with long-range van der Waals attractive interactions between the solute and the pore wall. Calculated values of α_1 for these two cases are also plotted in Figure 3. It is clear that the theoretical values of α_1 calculated with solute and pore wall van der Waals interactions fit the experimental data very well.

The basic principle underlying the effect of bulk solution concentration on the local distribution coefficient is that the lack of spherical symmetry inside the pore, due to interactions between the solute and the pore wall, causes the mean spacing, and hence, the mean interactions between particles within the pore to be different than in the bulk solution. Because of the effect of the pore wall, the mean particle-particle spacing inside the pore is much larger than in bulk solution and, hence, the mean particle-particle interactions inside the pore are weaker than in the bulk solution. Particle-particle interactions in the bulk solution tend to enhance the distribution of particles towards the pore solution leading to an increase in K_{eq} as concentration increases (that is, $\alpha_1 > 0$). Long-range attractive interactions between the particle and the pore wall tend to decrease the mean particle-particle intrapore spacing, leading to α_1 values which are smaller than those predicted with only steric interactions.

Table 5. Calculated Values for α_1

λ	α_1 Steric Interact.	α_1 Long-Range Interact. with $A = 5.0 \times 10^{-21}$ J
0.04	0.257	0.185
0.06	0.388	0.241
0.08	0.526	0.284
0.10	0.670	0.443
0.12	0.820	0.562
0.14	0.976	0.632
0.16	1.141	0.744
0.18	1.310	0.830
0.20	1.462	0.864

As discussed earlier, Batchelor separated the effect of solute concentration on bulk-phase diffusion into excluded volume (thermodynamic) and hydrodynamic contributions. When solutes are inside the pore, interactions between the solutes are more complicated than in bulk solution because of the effect of the pore wall. A comparison of the results in Figures 3 and 4 shows that the measured values of β_1 are similar in value to the measured values for the thermodynamic coefficients α_1. This is emphasized in Figure 4 where the experimentally determined values of β_1 are compared to the theoretical predictions for α_1. The virial coefficient α_1 accounts for excluded volume effects and is therefore analogous to the thermodynamic contribution described in Batchelor's analysis of the effect of solute-solute interactions on bulk-phase diffusion (which has a value of 8 in an unbounded fluid). The fact that our measured values of β_1 are close in value to the measured and predicted values of α_1 appears to indicate that the excluded volume effects dominate the effect of solute concentration on the intrapore diffusivity. However, the situation is clearly more complicated than this because it is obvious that the relationship between β_1 and λ is qualitatively different than the dependence of α_1 on λ. A more complete and quantitative interpretation of our data will need to wait for new theoretical developments which include solute-solute hydrodynamic interactions in small pores.

Polyethylene glycol

Negative values of α_1 and β_1 indicate that the effective diffusion coefficient of PEG decreases as solution concentration increases. Johansson et al. (1991) studied the diffusion of monodisperse fractions of PEG ($300 < \overline{M}_w < 4{,}000$) at different concentrations in κ-carrageenan and also found that effective diffusion coefficients decreased with increasing PEG concentration. The negative values of α_1 and β_1 may be explained by considering changes in the conformation of PEG that occur as concentration increases, a phenomenon that has been observed by others performing different types of measurements with PEG. From volumetric properties, Lepori and Mollico (1978) indicated that the most realistic picture of the PEG molecule in aqueous solutions is an "expanded" random coil of hydrated polymer. Israelachvili (1997) found that the properties of PEG depend on molecular weight and concentration. By measuring the intrinsic viscosity of PEG in water, Bailey and Callard (1959) concluded that the PEG polymer chains become entangled when the PEG concentration reached several wt. %. The PEG concentration of solutions used in this study ranged from 2 to 5 wt. %. From light scattering measurements of polyethylene oxide solutions prepared using carefully purified water, Devanand and Selser

(1990) found no evidence of aggregation and argue that the aggregation observed by others can be attributed to the effect of low concentrations of organic impurities on the thermodynamics of these solutions. In our experiments, the water used in preparing our solutions was distilled and filtered through a 0.1 μm membrane. However, no efforts were made to purify the polymer and it is quite possible that organic impurities may have been introduced into our solutions from the polymer samples. Whatever the driving force, it appears that aggregation was a factor in our PEG systems, leading to an increase in the effective Stokes-Einstein radius of the polymer as solution concentration was increased. If the mean dimensions of PEG increase as concentration increases, the steric limitations imposed by the pore wall also increase. This increase in the excluded volume near the pore wall can result in a decrease in the equilibrium partition coefficient as concentration increases (that is, $\alpha_1 < 0$). The intrapore diffusion coefficient is also expected to decrease as the PEG solute size increases, yielding negative values of β_1. These conformational changes can explain the apparent decrease in the effective diffusion coefficient of PEG as concentration increases.

It is important to emphasize here that the measured diffusion coefficients of dextran and PEG were found to be quite similar when measured under infinite dilution conditions (Shao, 2000; Shao and Baltus, 2000). The fact that the concentration dependence of the hindered diffusion of these two polymers is so clearly different indicates that the conformation of these two polymers is different and that this difference leads to drastically different responses to increases in solution concentration. This comparison illustrates that one must be cautious when predicting the behavior of one polymer from measurements on another.

As noted earlier, it was assumed that $\alpha_1 \beta_1 K_{\mathrm{eq},o} + \alpha_2 + \beta_2 K_{\mathrm{eq},o}^2 / 3 = \alpha_1 \beta_1 K_{\mathrm{eq},o}$ when determining values for the two first-order coefficients, α_1 and β_1 using Eq. 10. To justify this assumption, we rely on estimates for α_2 and β_2 garnered from the literature. Values for α_2 were estimated using approximations presented by Post and Glandt (1985) for a rigid, noninteracting spherical solute, values of which are predicted to be negative. A value for β_2 was estimated using the bulk solution prediction presented by Beenakker and Mazur (1982) ($\beta_2 = 0.91$). These calculations predict that $\alpha_1 \beta_1 K_{\mathrm{eq},o} > \alpha_2 + \beta_2 K_{\mathrm{eq},o}^2/3$, primarily because the negative values of α_2 are cancelled by the positive prediction for $\beta_2 K_{\mathrm{eq},o}^2/3$. Although these predictions for α_2 and β_2 are unlikely to be valid for our system, it is reasonable to expect that α_2 should be negative and β_2 positive, leading to some level of cancellation between α_2 and $\beta_2 K_{\mathrm{eq},o}^2/3$. The fact that the values for α_1 and β_1 show internal consistency with solutions of different concentration also provides support for our assumption that $\alpha_2 + \beta_2 K_{\mathrm{eq},o}^2/3 = 0$.

Conclusions

The diffusion rates of dextran and polyethylene glycol in track-etched polycarbonate membranes were experimentally investigated using solutions with sufficiently high concentration so that intermolecular interactions are expected to be important. A model that expresses the concentration dependence of both the equilibrium partition coefficient and the intrapore diffusivity with a first virial expansion in concentration was proposed to interpret the data. For each solute, experimental values of the first virial coefficient for partitioning and the first virial coefficient for intrapore diffusivity were found to be internally consistent with different solution concentrations and, for dextran, with molecular weight fractions.

For dextran, measured effective diffusion coefficients were observed to increase as solute concentration increases. Measured values of the first-order virial coefficient for equilibrium partitioning are smaller than those predicted for hard spheres subject only to steric interactions with each other and with the pore wall, but are in excellent agreement with values predicted when attractive van der Waals interaction between a hard sphere and the pore wall are included. The Hamaker constant used in the calculation of the van der Waals attractive interaction was determined from literature values for the individual materials and was consistent with the value found to explain diffusion coefficients measured at infinite dilution limits. The measured virial coefficient for the intrapore diffusivity of dextran was similar in magnitude to the virial coefficient for equilibrium partitioning, indicating that excluded volume effects appear to be a dominant factor on the effect of solute concentration on intrapore transport.

For the PEG, measured effective diffusion coefficients were observed to decrease as solute concentration increases. A possible explanation for this observation is that at high concentration, there is chain entanglement resulting in an increase in the effective molecular size and, hence, a decrease in the observed diffusion coefficient.

Acknowledgment

This study was supported by the National Institutes of Health under project No. 1 R15 GM51012-01.

Notation

b_1 = first interaction coefficient defined in Eq. 15
$b_1^{(S)}$ = first interaction coefficient for only steric interaction defined in Eq. 20
$b_1^{(LR)}$ = first interaction coefficient for long-range attractive interaction between solute and the pore wall defined in Eq. 21
D_{eff} = effective diffusion coefficient of solute in membrane (cm^2/s)
E = interaction energy between solute and the pore wall (J)
ℓ = length of pore (cm)
n = number of pores
U = pair potential acting between two particles (J)
β_1 = first virial coefficient for intrapore diffusivity defined in Eq. 7
β = dimensionless radial position of solute (r/r_p)
λ = solute-to-pore size ratio (r_s/r_p)
ϕ = time-averaged local particle volume fraction in the pore
ϕ_H^o = initial volume fraction of solute in the high concentration cell
$\phi_{L,\mathrm{meas}}$ = measured volume fraction of each collected sample
$\phi_{L,\mathrm{pred}}$ = volume fraction of each collected sample predicted using Eq. 10
ν_2 = specific volume of solute (mL/g)

Literature Cited

Anderson, J. L., and R. P. Adamski, "Solute Concentration Effects on Membrane Reflection Coefficients," *AIChE Symp. Ser.*, **79**, 84 (1983).

Anderson, J. L., and J. H. Brannon, ''Concentration Dependence of the Distribution Coefficient for Macromolecules in Porous Media,'' *J. Poly. Sci.: Polym. Phys. Ed.*, **19**, 405 (1981).
Bailey, F. E., Jr., and R. W. Callard, ''Some Properties of Poly(ethylene oxide) in Aqueous Solution,'' *J. Appl. Poly. Sci*., **1**, 56 (1959).
Batchelor, G. K., ''Brownian Diffusion of Particles with Hydrodynamic Interaction,'' *J. Fluid Mech*., **74**, 1 (1976).
Beenakker, C. W. J., and P. Mazur, ''Diffusion of Spheres in Suspension: Three-Body Hydrodynamic Interaction Effects,'' *Phys. Lett*., **91**, 290 (1982).
Berne, B., and R. Pecora, *Dynamic Light Scattering*, Wiley, New York, (1976).
Bhattacharjee, S., and A. Sharma, ''Lifshitz-van der Waals Energy of Spherical Particles in Cylindrical Pores,'' *J. Colloid Interface Sci*., **171**, 288 (1995).
Bleha, T., D. Bakos, and D. Berek, ''Estimation of Thermodynamic Quality of the Solvent from the Concentration Effect in Gel Permeation Chromatography of Polymer,'' *Polymer*, **18**, 897 (1977).
Brannon, J. H., and J. L. Anderson, ''Concentration Effects on Partitioning of Dextrans and Serum Albumin,'' *J. Poly. Sci.: Poly. Phys. Ed*., **20**, 857 (1982).
Cantow, M. J. R., et al., ''Sample Concentration Effect in Gel Permeation Chromatography,'' *J. Poly. Sci. Poly. Lett. Ed*., **4**, 707 (1966).
Chun, M. S., and R. J. Phillips, ''Electrostatic Partitioning in Slit Pores by Gibbs Ensemble Monte Carlo Simulation,'' *AIChE J*., **43**, 1194 (1997).
Deen, W. M., ''Hindered Transport of Large Molecules in Liquid-Filled Pores'' *AIChE J*., **33**, 1409 (1987).
Devanand, K., and J. C. Selser, ''Polyethylene Oxide Does Not Necessarily Aggregate in Water,'' *Nature*, **343**, 739 (1990).
Glandt, E. D., ''Distribution Equilibrium Between a Bulk Phase and Small Pores,'' *AIChE J*., **27**, 51 (1981).
Graessley, W. W., ''Polymer Chain Dimensions and the Dependence of Viscoelastic Properties on Concentration, Molecular Weight and Solvent Power,'' *Polymer*, **21**, 258 (1980).
Hamaker, H. C., ''The London-Van der Waals Attraction between Spherical Particles,'' *Physica*, **10**, 1058 (1937).
Hiemenz, P. C., and R. Rajagopalan, *Principles of Colloid and Surface Chemistry*, 3rd ed., Marcel Dekker, New York (1997).
Israelachvili, J., ''The Different Faces of Poly(ethylene glycol),'' *Proc. Nat. Acad. Sci*., **94**, 8378 (1997).
Johansson, L., C. Elvingson, and J.-E. Loftroth, ''Diffusion and Interaction in Gels and Solutions. 2. Experimental Results on the Obstruction Effect,'' *Macromol.*, **24**, 6019 (1991).
Lepori, L., and V. Mollica, ''Volumetric Properties of Dilute Aqueous Solutions of Poly(ethylene Glycols),'' *J. Poly. Sci*., *Poly. Phys. Ed*., **16**, 1123 (1978).
McQuarrie, D. A., *Statistical Mechanics*, Harper and Row, New York (1976).
Mitchell, B. D., and W. M. Deen, ''Theoretical Effects of Macromolecular Concentration and Charge on Membrane Rejection Coefficients, '' *J. Memb. Sci*., **19**, 75 (1984).
Mitchell, B. D., and W. M. Deen, ''Effects of Concentration on the Rejection Coefficients of Rigid Macromolecules in Track-Etch Membranes,'' *J. Colloid Interface Sci.*, **113**, 132 (1986).
Post, A. J., ''Solute Partitioning between a Micropore and a Bulk Solution: A Linear Density Functional Approach,'' *J. Colloid Interface Sci*., **129**, 451 (1989).
Post, A. J., and E. D. Glandt, ''Equilibrium Partitioning in Pores with Adsorbing Walls,'' *J. Colloid Interface Sci.*, **108**, 31 (1985).
Post, A. J., and D. A. Kofke, ''Fluids Confined to Narrow Pores: A Low-Dimensional Approach,'' *Phys. Rev. A*, **45**, 939 (1992).
Rudin, A., ''Concentration Effects in Gel-Permeation Chromatography,'' *J. Poly. Sci., A-1*, **9**, 2587 (1971).
Satterfield, C. N., C. K. Colton, B. D. Turckheim, and T. M. Copeland, ''Effect of Concentration on Partitioning of Polystyrene within Finely Porous Glass,'' *AIChE J*., **24**, 937 (1978).
Selim, M. S., and M. A. Al-Naafa, ''Brownian Diffusion of Hard Spheres at Finite Concentrations,'' *AIChE J*., **39**, 4 (1993).
Shao, J., ''The Effect of Solute Concentration on the Hindered Diffusion of Dextran and Polyethylene Glycol in Porous Membranes,'' PhD Diss., Clarkson Univ., Potsdam, NY (2000).
Shao, J. and R. E. Baltus, ''Hindered Diffusion of Dextran and Polyethylene Glycol in Porous Membranes,'' *AIChE J*., in press (2000).
Singh, S., K. C. Khulbe, T. Matsuura, and P. Ramamurthy, ''Membrane Characterization by Solute Transport and Atomic Force Microscopy,'' *J. Memb. Sci*., **142**, 111 (1998).

Manuscript received July 16, 1999, and revision received Jan. 31, 2000.